Major Article

Dysregulation of Epstein-Barr virus infection in hypomorphic *ZAP70* mutation

Akihiro Hoshino,[1, 2] Takehiro Takashima,[2] Kenichi Yoshida,[3] Akira Morimoto,[4] Yuta Kawahara,[4] Tzu-Wen Yeh,[2] Tsubasa Okano,[2] Motoi Yamashita,[2] Noriko Mitsuiki,[2] Kohsuke Imai,[5] Takashi Sakatani,[6] Atsuko Nakazawa,[7] Yusuke Okuno,[8] Yuichi Shiraishi,[9] Kenichi Chiba,[9] Hiroko Tanaka,[10] Satoru Miyano,[9, 10] Seishi Ogawa,[3] Seiji Kojima,[8] Tomohiro Morio,[2] and Hirokazu Kanegane[2]

[1]Department of Pediatrics, Graduate School of Medicine and Pharmaceutical Sciences, University of Toyama, Toyama, Japan

[2]Department of Pediatrics and Developmental Biology, Graduate School of Medical and Dental Sciences, Tokyo Medical and Dental University, Tokyo, Japan.

[3]Department of Pathology and Tumor Biology, Graduate School of Medicine, Kyoto University, Kyoto, Japan

[4]Department of Pediatrics, Jichi Medical University of Medicine, Shimotsuke, Japan

[5]Department of Community Pediatrics, Perinatal and Maternal Medicine, Graduate School of Medical and Dental Sciences, Tokyo Medical and Dental University, Tokyo, Japan

[6]Department of Diagnostic Pathology, Jichi Medical University Hospital, Shimotsuke, Japan

[7]Department of Pathology, National Center for Child Health and Development, Tokyo, Japan

[8]Department of Pediatrics, Nagoya University Graduate School of Medicine, Nagoya, Japan [9]Laboratory of DNA Information Analysis, Human Genome Center, Institute of Medical Science, The University of Tokyo, Tokyo, Japan

[10]Laboratory of Sequence Analysis, Human Genome Center, Institute of Medical Science, The University of Tokyo, Tokyo, Japan.

Corresponding author

Hirokazu Kanegane, MD, PhD

Department of Pediatrics and Developmental Biology

Graduate School of Medical and Dental Sciences, Tokyo Medical and Dental University

1-5-45 Yushima, Bunkyo-ku, Tokyo 113-8519, Japan

Telephone & Fax: +81-3-5803-5244

E-mail: hkanegane.ped@tmd.ac.jp

Running head: EBV infection in ZAP70 deficiency

Short summary

We identified a novel hypomorphic *ZAP70* mutation in a fatal Epstein-Barr virus (EBV)-associated lymphoproliferative disorder, and our study revealed that EBV-specific $CD8^+$ T cells and invariant NKT cells are critically involved in immune response against EBV infection.

Abstract

Background. Some patients with genetic defects develop Epstein-Barr virus (EBV)-associated lymphoproliferative disorder (LPD)/lymphoma as the main feature. Hypomophic mutations can cause different clinical and laboratory manifestations from null mutations in the same genes.

Methods. We sought to describe the clinical and immunologic phenotype of a 21-month-old boy having EBV-associated LPD who was in good health till then. A genetic and immunologic analysis was performed.

Results. Whole exome sequencing identified a novel compound heterozygous mutation of *ZAP70* c.703-1G>A and c.1674G>A. A small amount of the normal transcript was observed. Unlike ZAP70 deficiency which is previously described as severe combined immunodeficiency with non-functional $CD4^+$ T cells and absent $CD8^+$ T cells, the patient had slightly low numbers of $CD8^+$ T cells and a small amount of functional T cells. EBV-specific $CD8^+$ T cells and invariant NKT (iNKT) cells were absent. The T-cell receptor repertoire using next generation sequencing was significantly restricted.

Conclusions. Our patient shows that a hypomorphic mutation of *ZAP70* can lead to EBV-associated LPD and that EBV-specific $CD8^+$ T cells and iNKT cells are critically involved in immune response against EBV infection.

Key words

Epstein-Barr virus, hypomorphic mutation, lymphoproliferative disorder, T-cell receptor repertoire, whole exome sequencing, ZAP70

Epstein-Barr virus (EBV) infects the majority of population worldwide. Primary EBV infection is asymptomatic or occasionally causes infectious mononucleosis. Following primary infection, although EBV is not eliminated in memory B cells for the lifetime of the hosts, EBV is latently maintained being controlled by the host immune response [1]. In this setting, EBV-specific T cells play important roles [1-3]. Indeed, in human immunodeficiency virus-infected or post-transplant patients, impaired T cell response allows EBV-infected cells to become proliferating blasts, which can result in lymphoproliferative disease (LPD) or lymphoma [4, 5]. Although humanized mouse models have partially contributed to reveal immune response against EBV infection [6], the details remain unclear. Some types of genetic defects are known and recently described for developing EBV-associated LPD/lymphoma as the main feature [7-11]. These disorders include signaling lymphocytic activation molecule-associated protein (SAP) deficiency [7, 8], interleukin-2 inducible tyrosine kinase (ITK) deficiency [9], CD27 deficiency [10], X-linked immunodeficiency with magnesium defect, EBV infection, and neoplasia (XMEN) disease [11]. These primary immunodeficiencies (PIDs) provided new insights of roles of T-cell receptor (TCR) or associated co-stimulatory signals and added evidences of critically involvement of invariant natural killer T (iNKT) cells in immune response against EBV infection [2, 3].

Here we describe an EBV-LPD patient associated with a hypomorphic mutation of *zeta-chain associated protein kinase, 70 kd* (*ZAP70*), who showed pivotal roles of T-cell recognition and iNKT cells in the control of EBV. ZAP70 is a non-receptor tyrosine kinase which is a key component of the TCR signal transduction pathway [12, 13]. ZAP deficiency is previously described as severe combined immunodeficiency (SCID) with non-functional $CD4^+$ T cells and absent $CD8^+$ T cells [14]. The patient was in good health until EBV infection with a few functional $CD4^+$ and $CD8^+$ T cells. However, dysregulation of EBV infection was revealed by cytomolecular analysis including TCR repertoire analysis using next generation sequencing (NGS).

MATREIALS AND METHODS

Ethical Considerations

The informed consent was obtained from the patient's parents. The study was conducted in accordance with the Helsinki Declaration and was approved by the ethics board of the University of Toyama and Tokyo Medical and Dental University.

Genetic Analysis

WES was performed using genomic DNA from whole blood of the patient and his parents as described elsewhere [15]. In brief, exome capture was carried out using a SureSelect Human All Exon V5 kit (Agilent technologies, Santa Clara, CA), and massively-parallel sequencing was performed using a HiSeq 2000 platform (Illumina, San Diego, CA) with 100 bp-paired-end reads. The data were processed with an in-house constructed analysis pipeline, which conducted the alignment of the reads with Burrows-Wheeler aligner 0.5.8 [16], counting of variant allele numbers with Samtools [17], and annotation with ANNOVAR [18]. Identified variants were filtered using dbSNP131, an in-house SNP database, and the Human Genetic Variation Database (http://www.genome.med.kyoto-u.ac.jp/SnpDB/). Predicted functional effects of variants were determined using SIFT [19], PhyloP [20], PolyPhen2 [21], and MutationTaster [22]. In order to validate the results, polymerase chain reaction (PCR) using primers listed in Supplementary Table 1 and Sanger sequencing was performed.

RT-PCR and Detection of Splicing Product

RNA was extracted from peripheral blood mononuclear cells (PBMCs) according to standard methods and cDNA was prepared using SuperScript VILO (Invitrogen, Carlsbad, CA). PCR was performed using cDNA. The PCR products were cloned using TOPO TA cloning kit (Life Technologies, Carlsbad, CA) and independent clones were sequenced. Primers were listed in Supplementary Table 1.

Flow Cytometry

PBMCs were stained with fluorochrome-conjugated antibodies. Stained cells were analyzed using BD LSRFortessa (BD Biosciences, San Jose, CA) and the data processed using FlowJo software (Tree Star Inc., Ashland, OR). For lymphocyte phenotyping, monoclonal antibodies used to stain cell surface were listed in Supplementary Table 2. For EBV-specific $CD8^+$ T cells, PBMCs were incubated with Clear Back (MBL, Nagoya, Japan) to block the Fc receptors, and stained with HLA-A*24:02 EBV mix Tetramer-phycoerythrin (PE) (MBL), followed by PE-Vio770-conjugated anti-CD8 (clone BW135/80, Miltenyi Biotec, Bergisch Gladbach, Germany). The patient had HLA-A*24:02. For intracellular ZAP70 staining, PBMCs were labeled with VioGreen-conjugated anti-CD3 (clone BW264/56, Miltenyi Biotec), VioBlue-conjugated anti-CD4 (clone M-T466, Miltenyi Biotec) and PE-Vio770-conjugated anti-CD8. Then, cells were fixed and permeabilized with Fixation/Permeabilization kit (eBioscience, San Diego, CA), washed in permeabilization buffer (eBioscience) and stained with PE-conjugated anti-ZAP70 (clone 1E7.2, eBioscience).

Functional Analysis

For calcium flux analysis, PBMCs were loaded with 2 µM Fluo-4 AM (Life Technologies) for 45 min at 37 °C and stained for CD4 and CD8. Cells were stimulated with mouse anti-human CD3 (1 µg/ml; clone UCHT1, BD Pharmingen, San Diego, CA) and goat anti-mouse antibodies (BD Pharmingen), or ionomycin (8 µg/ml; Life technologies). The analysis was performed by flow cytometry and kinetic plots using FlowJo software. For T-cell proliferation analysis, PBMCs were labeled with CFSE (3 µM; eBioscience) for 5 min at room temperature and stimulated for 4 days with anti-CD3/CD28 activating Dynabeads (Life Technologies, Oslo, Norway), or phorbol myristate acetate (PMA, 10 ng/mL; Sigma-Aldrich) and ionomycin (0.25 µg/mL; Sigma-Aldrich). Then, cells were stained for CD4 and CD8, and analyzed by flow cytometry.

Immunoblot and immunoprecipitation analysis

The entire coding region of wild-type (WT) *ZAP70* cDNA was subcloned in a pcDNA3 vector (Invitrogen, Waltham, MA). The mutant ZAP70 expression vectors were generated by site-directed mutagenesis. The plasmids containing WT or mutant *ZAP70* genes were transfected into P116 cells using Lipofectamine LTX Reagent (Thermo Fisher Scientific, Waltham, MA), according to the manufacturer's protocol. At 24 h after transfection, the cells were subjected. For immunoblot analysis, cells were stimulated with mouse anti-human CD3 (1 µg/ml) and goat anti-mouse antibodies for 5 minutes. For immunoprecipitation analysis, Dynabeads M-280 sheep anti-rabbit IgG (Life Technologies, Carlsbad, CA) was used. Immunoblot and immunoprecipitation analysis was performed using following antibodies; anti-ZAP70 (ab134509, Abcam, Cambridge, UK), anti-SLP76 (ab109254, Abcam), anti-pY113 SLP76 (ab75990, Abcam) and anti-CD3ζ (ab226475, Abcam).

TCR Repertoire Analysis

cDNA from PBMCs was amplified using the HTBI-M reagent system (iRepertoire Inc., Huntsville, AL) according to the manufacturer's protocol, which include nested primers targeting each of the V and J elements for the first round of PCR and communal primers for the second round of PCR. After gel purification, the resulting product were sequenced using a MiSeq platform (Illumina). The data were processed with a provided pipeline (iRepertoire Inc.). For each sequence, copy number, complementary determining region 3 (CDR3) length, V and J usage, N addition and V and J trimming were determined. Shannon entropy was calculated [23].

TRECs Analysis

T-cell receptor excision circles (TRECs) quantification was performed by real-time PCR using genomic DNA from whole blood of the patient as previously described [24].

Quantitation of DNA Copy Number

In order to determine the ratio of X and Y chromosome, the copy number of *IL2RG* and *SRY*, which are on X and Y chromosome, respectively, were measured. Droplet digital PCR (ddPCR) was performed using QX200 Droplet Digital PCR System (Bio-Rad Laboratories, Hercules, CA). The primers and the hydrolysis probes were listed in Supplementary Table 1. The *IL2RG* probes were labeled with HEX and *SRY* probe was labeled with FAM.

Immunohistochemical Staining

Pathological analysis was performed on cervical lymph node tissue. For immunohistochemistry, antibodies against cytoplasmic CD3, CD4, CD8, CD20 (Nichirei Biosciences, Tokyo, Japan), latent membrane protein 1 (LMP1, clone CS.1-4, DAKO, Tokyo, Japan), Epstein-Barr virus nuclear 2 (EBNA2, clone PE2, DAKO) were used. EBV genome was detected by *in situ* hybridization using EBV-encoded RNA signals (EBERs, EBER PNA probe, DAKO).

RESULTS

Clinical Features

A 21-month-old boy presented with fever, systemic lymphadenopathy and facial paralysis. The patient was found to have enlarged spleen and EBV viremia (24,000 copies/10^6 cells). He was born to nonconsanguineous Japanese parents and was in good health until he was admitted. He was immunized with live measles-rubella and BCG without adverse effect. His parents and 3 elder siblings were healthy except for the second brother. The brother died of acute encephalopathy at the age of 6 years, whose $CD8^+$ T-cell counts were within normal range. The patient was diagnosed with EBV-associated LPD, as described below. The patient temporarily responded to 2 mg/kg/day of prednisolone, however, he developed mass lesions in his brain, liver, kidneys and lungs at 24 months of age. They were refractory to the multi-agent chemotherapy including anti-CD20 antibodies, cyclophosphamide, vincristine, pirarubicin, etoposide, high-dose methotrexate (MTX), high-dose cytarabine (Ara-C) and intrathecal injection of MTX, Ara-C and hydrocortisone. Subsequently the mass lesion also appeared in his heart, which led to his death due to fetal atrioventricular block at 27 months of age.

Pathological Findings

Figure 1 shows histologic findings of the cervical lymph node before chemotherapy. Normal architecture of the lymph node was partially effaced and large and medium-sized lymphoid cell proliferation was observed. Large lymphoid cells were positive for CD20 and EBERs, while medium-sized lymphoid cells were positive for cytoplasmic CD3 and CD8 or CD4. Staining with EBNA2 and LMP1was positive, which indicated type III latency pattern.

Immunodeficiency

The immunological data are summarized in Table 1. Total lymphocyte counts were normal, but T-cell counts were low with decreased, but not absent, $CD8^+$ T-cell counts (5%). Interestingly, $CD8^+$ T-cell percentages were increased to 12% in total lymphocytes with 1.2 of CD4/CD8 ratio, when the patient was 24 months old. B- and NK-cell counts were almost within normal range. Before intravenous immunoglobulin, serum IgG, IgA and IgM levels were elevated. He had protective titers of measles and rubella antibodies as postvaccination titers; however, antibodies for EBV viral capsid antigen (VCA) IgG, VCA IgM and EBNA antibodies were negative 3 weeks after onset of symptoms.

The immunophenotypic analysis of T-cell subpopulations revealed markedly decreased proportions of both naïve $CD4^+$ and $CD8^+$ T cells. We also found increased $TCR\gamma\delta^+$ T-cell and $TCR\alpha\beta^+$ double negative T-cell counts, and decreased iNKT cell counts, suggesting aberrant development of T cells. Especially, iNKT cells were near to absent (Figure 2A). EBV-specific $CD8^+$ T-cell counts were severely diminished (Figure 2B), consisting with the histologic findings with latency type III [26]. Because those data were measured after chemotherapy, to distinguish whether the cause of absence of iNKT cells is the chemotherapy or the underlying disease, we measured iNKT-cell counts in two groups; healthy controls and disease controls during or after chemotherapy and/or anti-CD20 antibodies

administration. iNKT-cells counts were not different in those two groups, strongly suggesting that the patient had the underlying disease (Supplementary Figure 1). TREC levels were negative.

Identification of *ZAP70* Mutation

The immunological data suggested that the patient have a specific susceptibility to EBV. We hypothesized that this susceptibility was caused by a single gene disorder, and performed WES using DNA samples from the patient and his parents. As a result of filtering called variants, 5 candidate variants were identified including novel 2 variants which are compound heterozygous *ZAP70* mutation c.703-1G>A and c.1674G>A (p.Met558Ile) (Supplementary Table 3). The other 3 variants were not considered as disease causing genes because that these genes were not related to immune system and the variants were not predicted as damaging using functional prediction algorithms. We confirmed the compound heterozygous *ZAP70* mutations by Sanger sequencing (Figure 3A, B and Supplementary Figure 2A). The c.703-1G>A mutation was present in his father and the c.1674G>A mutation was present in his mother (Figure 3B). Sequencing of RT-PCR product from RNA sample revealed a splice variant lacking exon 6 (Supplementary Figure 2B). Exon 6 includes binding site to CD3 immunoreceptor tyrosine-based activation motifs (Supplementary Figure 2C), and Met558 is highly conserved (Supplementary Figure 2D). These findings suggest the compound heterozygous *ZAP70* mutation c.703-1G>A and c.1674G>A is disease causing.

Reduced Expression of ZAP70 Protein and Functional Defects in Mutant ZAP70

ZAP70 protein expression in T cells was analyzed using flow cytometry. ZAP70 expression was reduced in $CD4^+$ and $CD8^+$ T cells from the patient (Figure 3C). There is no difference in ZAP70 expression between $CD4^+$ and $CD8^+$ T cells in the patient.

To determine the impact of ZAP70 mutants, ZAP70-deficient Jurkat P116 cells were transiently transduced with a vector which encodes for WT ZAP70 ($ZAP70^{WT}$), Met558Ile variant ($ZAP70^{M558I}$) or exon 6-deleted ZAP70 ($ZAP70^{\Delta exon\ 6}$). The expression of 2 mutant ZAP70 proteins were reduced, suggesting the degradation of the mutant protein (Figure 4A). We then analyzed TCR signaling downstream of ZAP70. Whereas CD3 cross-linking induced significant phosphorylation of SLP76 in ZAP70WT-transfected cells, those were significantly diminished in $ZAP70^{M558I}$ or $ZAP70^{\Delta exon\ 6}$-transfected cells (Figure 4A). Furthermore, immunoprecipitation analysis showed that $ZAP70^{\Delta exon\ 6}$ protein failed to bind CD3ζ chain (Figure 4B). These results indicate that the identified ZAP70 mutations are loss-of function due to their inability to transduce TCR signaling.

Detection of Wild Type Allele

Although the patient had compound heterozygous *ZAP70* mutations and reduced expression of ZAP70, there were several different findings from typical ZAP70 deficiency reported previously; i.e. not meeting the criteria of SCID (http://esid.org/Working-Parties/Registry/Diagnosis-criteria) and milder $CD8^+$ T cell lymphopenia. WES revealed the *ZAP70* mutations with 50% of allele frequency, and ddPCR revealed the X and Y chromosome ratio of 1:1, which did not suggest reversion mosaicism or maternal T-cell engraftment. In order to explore the cause of the hypomorphic phenotype, we hypothesized that a small amount of normal splicing might occur despite the splice site mutation. We cloned PCR products from cDNA spanning exon 3 to 14 of *ZAP70* and analyzed 45 independent clones by Sanger sequencing (Supplementary Figure 2E). Twenty clones were derived from aberrant splicing without exon 6, and 22

clones had missense mutation (c.1674G>A). The most remarkable result is that 3 clones were derived from normal splicing and did not have missense mutation (c.1674G>A).

Assessment of Lymphocyte Function

Signal transduction through the TCR/CD3 complex was examined in each $CD4^+$ or $CD8^+$ T-cell populations. First, TCR-mediated calcium mobilization was analyzed (Figure 5A, B). CD3 cross-linking induced a small and delayed free intracellular Ca^{2+} increases in the patient's $CD4^+$ and $CD8^+$ T cells. In contrast, ionomycin, which is non-TCR-mediated stimulation, induced free intracellular Ca^{2+} increases to the same degree of the control T cells. Second, T-cell proliferation after stimulation of the TCR was analyzed (Figure 5C, D). While PMA/ionomycin induced sufficient proliferation of patient T cells, anti-CD3/CD28 induced no proliferation of most T cells and sufficient proliferation of a few but sufficient number of T cells, especially $CD4^+$ T cells. These results demonstrate that most T cells are non-functional but a small amount of T cells are normally functional, consisting with the detection of wild type allele.

TCR Repertoire

The existence of hypofunctional T cells made us expect the slight skewing of TCR repertoire as previously described in typical ZAP70 deficiency patients [14]. TCR CDR3 sequences were analyzed using NGS. *TRBV* usage and CDR3 length were slightly skewed (Supplementary Figure 3A, B, C). Unexpectedly, T cells from the patient had significantly skewed V-J combinations with expansion of *TRBV6-5*/*TRBJ2-7*, *TRBV30*/*TRBJ1-2*, *TRBV18*/*TRBJ2-7* and *TRBV6-6*/*TRBJ2-7* (Supplementary Figure 4A). The reduced diversity and uneven distribution were observed (Supplementary Figure 4B, C). Junctional diversity was largely maintained (Supplementary Figure 3D).

DISCUSSION

We identified novel hypomorphic mutations of *ZAP70*, and the patient did not manifest SCID but EBV-associated LPD most likely following primary EBV infection. His laboratory findings indicated that impaired immunity against EBV might be associated with the development of LPD.

There are broadly similar laboratory findings between our patient and PIDs predisposed to EBV-associated LPD/lymphoma previously described. First, T cells especially naïve T cells are decreased, but not absent, and TCR or associated co-stimulatory signals are impaired. Other T-cell immunodeficiencies present different clinical manifestations. PIDs without T cells most often contract other infectious diseases, which are life-threatening, before EBV infections [27]. Although SCID patients can develop EBV-associated LPD/lymphoma, it is rare as a main feature [28]. PIDs with impaired lymphocyte cytotoxicity, represented by familial hemophagocytic lymphohistiocytosis (HLH), develop fulminant infectious mononucleosis (FIM) or HLH due to an uncontrolled overwhelming hypercytokinemia produced by activated $CD8^+$ T cells and NK cells [8]. SAP deficiency patients often develop FIM. The reason can be partially explained by the pathology of SAP deficiency including reduced $CD8^+$ T cell and NK cell cytotoxicity [8]. ZAP70 plays a pivotal role in TCR signal transduction, which is not directly related to lymphocyte cytotoxicity [12, 13]. In our patient, the development of EBV-associated LPD may have resulted from a limited resistance against the pathogens including live vaccine strains and impaired recognition of EBV-infected cells. Lack of EBV-specific $CD8^+$ T cells and negative titers of EBV antibodies support globally impaired T-cell recognition of EBV antigen.

Second, iNKT-cell counts are remarkably decreased. Reduced number of iNKT cells has been reported in SAP deficiency [7, 8], ITK deficiency [9], CD27 deficiency [10], Coronin-1A deficiency [29], and cytidine 5' triphosphate synthase 1 (CTPS1) deficiency [30]. iNKT cells can directly and rapidly

recognize EBV-infected cells through CD1d-mediated activation, and mediate direct cytotoxicity, which is especially critical during the earlier stage of EBV-infection [31]. iNKT cells are indirectly responsible for controlling EBV infection through NK-cell, T-cell and dendritic-cell activation by the production of IFN-γ and IL-2 [32]. ZAP70 is required for iNKT-cell development during the positive selection, and iNKT cells are absent in *Zap70* null mice [33]. Although the counts of iNKT cells in human ZAP70 deficiency is controversial [3, 34], these findings can help explain the remarkably decreased iNKT cells in the patient.

The third similar manifestations between our patient and PIDs predisposed to EBV-associated LPD/lymphoma is that B-cell counts and development are normal or less impaired. The majority of EBV-infected cells is B cells, and the presence of B cells is important for EBV-infection [1]. Dysgammaglobulinemia is often observed, but it is result from impaired T-cell function or EBV infection by itself [7-9, 29, 30].

Hypomorphic ZAP70 mutation resulted in different clinical and laboratory manifestations from those of null mutation. The similar findings have been described in *CORON1A* gene. While loss of function mutations of *CORON1A* are associated with $T^-B^+NK^+$ SCID [35], hypomorphic mutations lead to PID predisposed to EBV-associated LPD/lymphoma [29]. Hypomorphic mutations due to normal splicing have been reported in some diseases [36, 37], including one *ZAP70* patient [38]. The reported patient had had recurrent infections since infancy, and at last in the follow-up, at 9 years of age, he was well without transplantation. Severe EBV infection was not observed, however; he developed severe varicella-zoster virus infection. Although the reason of difference of susceptibility to EBV between our patient and the reported patient remains unclear, it may reflect clinical exposure or the impact of genetic defects including iNKT-cell differentiation and TCR signal transduction.

TCR repertoire analysis in great detail using NGS showed significant restriction of the TCR repertoire with reduced diversity and uneven distribution in the patient, indicating the abnormal T-cell

generation and the nonrandom usage of V, D and J elements. These results confirm and extend previous findings of ZAP70 involvement at the immature single positive thymocyte stage to the double positive thymocyte stage [14]. Restriction of the TCR repertoire might contribute that EBV-specific CDR3 sequences could not be accidentally produced, whereas other pathogen-specific CDR3 sequences could be produced including measles and rubella. This hypothesis was supported by the observation that EBV-specific antibodies were negative whereas measles and rubella-specific antibodies were positive in the patient. If many antigen-specific CDR3 sequences will be known across a diverse HLA type, this analysis could be used to evaluate antigen-specific T cells [39-42].

ZAP70 alterations have a wide spectrum of clinical features. While loss of function mutations of *ZAP70* lead to SCID [12], hypomorphic mutations of *ZAP70* seem to be associated with the autoimmune disease [43, 44]. We identified novel hypomorphic mutations of *ZAP70* and described a selective dysregulation of EBV infection. Our findings extend the spectrum of clinical features of *ZAP70* alterations and indicated pivotal roles of T-cell recognition and iNKT cells in immune response against EBV.

Acknowledgements

We thank Dr. Hideki Muramatsu for the professional technical assistance.

Financial support

This work was supported by the Research on Measures for Intractable Disease Project, and the grants from Ministry of Education, Culture, Sports, Science and Technology of Japan (JSPS KAKENHI: 26461570); and the Ministry of Health, Labour and Welfare of Japan (H26-Nanchi-071).

Potential conflicts of interest

All authors: No reported conflicts.

References

1. Rickinson AB, Long HM, Palendira U, Münz C, Hislop AD. Cellular immune controls over Epstein-Barr virus infection: new lessons from the clinic and the laboratory. Trends Immunol **2014**; 35: 159-69.

2. Parvaneh N, Filipovich AH, Borkhardt A. Primary immunodeficiencies predisposed to Epstein-Barr virus-driven haematological diseases. Br J Haematol **2013**; 162: 573-86.

3. Palendira U, Rickinson AB. Primary immunodeficiencies and the control of Epstein-Barr virus infection. Ann N Y Acad Sci **2015**. [Epub ahead of print]

4. Petrara MR, Freguja R, Gianesin K, Zanchetta M, De Rossi A. Epstein-Barr virus-driven lymphomagenesis in the context of human immunodeficiency virus type 1 infection. Front Microbiol **2013**; 4: 311.

5. Nourse JP, Jones K, Gandhi MK. Epstein-Barr Virus-related post-transplant lymphoproliferative disorders: pathogenetic insights for targeted therapy. Am J Transplant **2011**; 11: 888-95.

6. Chijioke O, Müller A, Feederle R, et al. Human natural killer cells prevent infectious mononucleosis features by targeting lytic Epstein-Barr virus infection. Cell Rep **2013**; 5: 1489-98.

7. Booth C, Gilmour KC, Veys P, et al. X-linked lymphoproliferative disease due to

SAP/SH2D1A deficiency: a multicenter study on the manifestations, management and outcome of the disease. Blood **2011**; 117: 53-62.

8. Yang X, Miyawaki T, Kanegane H. SAP and XIAP deficiency in hemophagocytic lymphohistiocytosis. Pediatr Int **2012**; 54: 447-54.

9. Ghosh S, Bienemann K, Boztug K, Borkhardt A. Interleukin-2-inducible T-cell kinase (ITK) deficiency - clinical and molecular aspects. J Clin Immunol **2014**; 34: 892-9.

10. van Montfrans JM, Hoepelman AI, Otto S, et al. CD27 deficiency is associated with combined immunodeficiency and persistent symptomatic EBV viremia. J Allergy Clin Immunol **2012**; 129: 787-93.

11. Li FY, Chaigne-Delalande B, Su H, Uzel G, Matthews H, Lenardo MJ. XMEN disease: a new primary immunodeficiency affecting Mg2+ regulation of immunity against Epstein-Barr virus. Blood **2014**; 123: 2148-52.

12. Fischer A, Picard C, Chemin K, Dogniaux S, le Deist F, Hivroz C. ZAP70: a master regulator of adaptive immunity. Semin Immunopathol **2010**; 32: 107-16.

13. Wang H, Kadlecek TA, Au-Yeung BB, et al. ZAP-70: an essential kinase in T-cell signaling. Cold Spring Harb Perspect Biol **2010**; 2: a002279.

14. Roifman CM, Dadi H, Somech R, Nahum A, Sharfe N. Characterization of ζ-associated protein, 70 kd (ZAP70)-deficient human lymphocytes. J Allergy Clin Immunol **2010**; 126: 1226-33.

15. Kunishima S, Okuno Y, Yoshida K, et al. ACTN1 mutations cause congenital macrothrombocytopenia. Am J Hum Genet. **2013**; 92: 431-8.

16. Li H, Durbin R. Fast and accurate short read alignment with Burrows-Wheeler transform. Bioinformatics **2010**; 26: 589-95.

17. Li H, Handsaker B, Wysoker A, et al. The Sequence Alignment/Map format and SAMtools. Bioinformatics **2009**; 25: 2078-9.

18. Wang K, Li M, Hakonarson H. ANNOVAR: functional annotation of genetic variants from high-throughput sequencing data. Nucleic Acids Res **2010**; 38: e164.

19. Kumar P, Henikoff S, Ng PC. Predicting the effects of coding non-synonymous variants on protein function using the SIFT algorithm. Nat Protoc **2009**; 4: 1073-81.

20. Pollard KS, Hubisz MJ, Rosenbloom KR, Siepel A. Detection of nonneutral substitution rates on mammalian phylogenies. Genome Res **2010**; 20: 110-21.

21. Adzhubei IA, Schmidt S, Peshkin L, et al. A method and server for predicting damaging missense mutations. Nat Methods **2010**; 7: 248-9.

22. Schwarz JM, Rödelsperger C, Schuelke M, Seelow D. MutationTaster evaluates disease-causing potential of sequence alterations. Nat Methods **2010**; 7: 575-6.

23. Yu X, Almeida JR, Darko S, et al. Human syndromes of immunodeficiency and dysregulation are characterized by distinct defects in T-cell receptor repertoire development. J Allergy Clin Immunol **2014**; 133: 1109-15.

24. Morinishi Y, Imai K, Nakagawa N, et al. Identification of severe combined immunodeficiency by T-cell receptor excision circles quantification using neonatal guthrie cards. J Pediatr **2009**; 155: 829-33.

25. Stiehm ER, Fudenberg HH. Serum levels of immune globulins in health and disease: a survey. Pediatrics **1966**; 37: 715-27.

26. Ok CY, Li L, Young KH. EBV-driven B-cell lymphoproliferative disorders: from biology, classification and differential diagnosis to clinical management. Exp Mol Med **2015**; 47: e132.

27. Notarangelo LD. Primary immunodeficiencies. J Allergy Clin Immunol **2010**; 125 (2 Suppl 2): S182-94.

28. Newell A, Dadi H, Goldberg R, Ngan BY, Grunebaum E, Roifman CM. Diffuse large B-cell lymphoma as presenting feature of Zap-70 deficiency. J Allergy Clin Immunol **2011**; 127: 517-20.

29. Moshous D, Martin E, Carpentier W, et al. Whole-exome sequencing identifies Coronin-1A deficiency in 3 siblings with immunodeficiency and EBV-associated B-cell lymphoproliferation. J Allergy Clin Immunol **2013**; 131: 1594-603.

30. Martin E, Palmic N, Sanquer S, et al. CTP synthase 1 deficiency in humans reveals its central role in lymphocyte proliferation. Nature **2014**; 510: 288-92.

31. Chung BK, Tsai K, Allan LL, et al. Innate immune control of EBV-infected B cells by invariant natural killer T cells. Blood **2013**; 122: 2600-8.

32. Priatel JJ, Chung BK, Tsai K, Tan R. Natural killer T cell strategies to combat Epstein-Barr virus infection. Oncoimmunology **2014**; 3: e28329.

33. Iwabuchi K, Iwabuchi C, Tone S, et al. Defective development of NK1.1+ T-cell antigen receptor alphabeta+ cells in zeta-associated protein 70 null mice with an accumulation of

NK1.1+ CD3- NK-like cells in the thymus. Blood **2001**; 97: 1765-75.

34. Hauck F, Blumenthal B, Fuchs S, Lenoir C, Martin E, Speckmann C, et al. SYK expression endows human ZAP70-deficient CD8 T cells with residual TCR signaling. Clin Immunol **2015**; 161: 103-9.

35. Shiow LR, Roadcap DW, Paris K, et al. The actin regulator coronin 1A is mutant in a thymic egress-deficient mouse strain and in a patient with severe combined immunodeficiency. Nat Immunol **2008**; 9: 1307-15.

36. Karakawa S, Okada S, Tsumura M, et al. Decreased expression in nuclear factor-κB essential modulator due to a novel splice-site mutation causes X-linked ectodermal dysplasia with immunodeficiency. J Clin Immunol **2011**; 31: 762-72.

37. Sobacchi C, Pangrazio A, Lopez AG, et al. As little as needed: the extraordinary case of a mild recessive osteopetrosis owing to a novel splicing hypomorphic mutation in the TCIRG1 gene. J Bone Miner Res **2014**; 29: 1646-50.

38. Picard C, Dogniaux S, Chemin K, et al. Hypomorphic mutation of ZAP70 in human results in a late onset immunodeficiency and no autoimmunity. Eur J Immunol **2009**; 39: 1966-76.

39. Miconnet I, Marrau A, Farina A, et al. Large TCR diversity of virus-specific CD8 T cells provides the mechanistic basis for massive TCR renewal after antigen exposure. J Immunol **2011**; 186: 7039-49.

40. Iancu EM, Corthesy P, Baumgaertner P, et al. Clonotype selection and composition of human CD8 T cells specific for persistent herpes viruses varies with differentiation but is stable over time. J Immunol **2009**; 183: 319-31.

41. Venturi V, Chin HY, Asher TE, et al. TCR beta-chain sharing in human CD8+ T cell responses to cytomegalovirus and EBV. J Immunol **2008**; 181: 7853-62.

42. Price DA, Brenchley JM, Ruff LE, et al. Avidity for antigen shapes clonal dominance in CD8+ T cell populations specific for persistent DNA viruses. J Exp Med **2005**; 202: 1349-61.

43. Turul T, Tezcan I, Artac H, et al. Clinical heterogeneity can hamper the diagnosis of patients with ZAP70 deficiency. Eur J Pediatr **2009**; 168: 87-93.

44. Haluk Akar H, Patiroglu T, Akyildiz BN, et al. Silent brain infarcts in two patients with zeta chain-associated protein 70kDa (ZAP70) deficiency. Clin Immunol **2015**; 158: 88-91.

Table I. Immunophenotyping of the patient

Parameter, units		Before treatment (21 months)	3 months after last chemotherapy (24 months)	Normal values†
Lymphocytes, /μL		4480	640	3600-8900
T cells, % (/μL)	$CD3^+$/Lym	34 (1520)	35 (220)	59-72 (2100-6400)
Helper T cells, % (/μL)	$CD4^+$/Lym	27 (1210)	14 (88)	38-54 (1400-4800)
Naïve $CD4^+$ T cells, %	$CD45RA^+/CD3^+CD4^+$	ND	4	77-89
Memory $CD4^+$ T cells, %	$CD45RO^+/CD3^+CD4^+$	ND	95	11-23
Recent thymic emigrants, %	$CD31^+/CD3^+CD4^+CD45RA^+$	ND	31	84-96
T follicular helper cells, %	$CD45RO^+CXCR5^+/CD3^+CD4^+$	ND	3	1-4

Regulatory T cells, %	$CD25^+CD127^-/CD3^+CD4^+CCR4^+$	ND	13	15-31
Cytotoxic T cells, % (/μL)	$CD8^+$/Lym	5 (220)	12 (74)	7-23 (390-2000)
Naïve $CD8^+$ T cells, %	$CD45RA^+/CD3^+CD8^+$	ND	4	78-91
Memory $CD8^+$ T cells, %	$CD45RO^+/CD3^+CD8^+$	ND	96	9-22
Central memory T cells, %	$CD62L^+CCR7^+/CD3^+CD8^+CD45RO^+$	ND	4	37-62
Effector memory T cells, %	$CD62L^-CCR7^-/CD3^+CD8^+CD45RO^+$	ND	61	10-30
TCRδγ T cells, %	$TCR\alpha\beta^-TCR\gamma\delta^+/CD3^+$	ND	20	1-13
Double negative T cells, %	$CD4^-CD8^-/CD3^+TCR\alpha\beta^+$	ND	21	1-2
invariant NKT cells, %	TCR $V\alpha24^+$TCR $V\beta11^+/CD3^+$	ND	0.00	0.01-0.12
B cells, % (/μL)	$CD19^+CD20^+$/Lym	36 (1610)	2 (14)*	8-22 (470-2000)
NK cells, % (/μL)	$CD16^+CD56^+$/Lym	27 (1210)	39 (250)	1-10 (100-1000)
IgG, g/L		16.01		5.53-9.71‡

IgA, g/L	1.82	0.26-0.74‡
IgM, g/L	2.82	0.35-0.81‡
Measles IgG, IU/mL	2200 (protective)	
Rubella IgG, IU/mL	93.0 (protective)	
EBV VCA IgM	<10	
EBV VCA IgG	<10	
EBNA antibodies	<10	
TREC, copies/μg DNA	Negative	3.5-8.1 × 10^3§

ND, not determined; TCR, T-cell receptor; NKT, natural killer T; EBV, Epstein-Barr virus; VCA, viral capsid antigen; EBNA, Epstein-Barr nuclear antigen; TREC, T-cell receptor excision circle.

* 3 months after last anti-CD20 antibodies.

† Age-matched normal values in Japanese as established by the performing laboratory.

‡ Reference 25.

§ Reference 24.

Figure legends

Figure 1. Pathological findings of the lymph node. A, Normal architecture of the cervical lymph node is partially effaced and large and medium-sized lymphoid cell proliferation is observed (hematoxylin-eosin stain, 100×). B and C, Most of large lymphoid cells were positive for EBER (B, 400×) and EBNA2 (C, 400×). D, Few large lymphoid cells were positive for LMP1 (400×).

Figure 2. iNKT cells and EBV-specific $CD8^+$ T cells. A, TCR $V\alpha24^+$ $V\beta11^+$ iNKT cells gated on $CD3^+$ T cells (left, healthy control subject; right, patient). B, HLA-A*24:02 EBV mix $Tetramer^+$ EBV-specific cells gated on $CD8^+$ T cells (left, healthy control subject; right, patient).

Figure 3. Genetic analysis of compound heterozygous mutation of *ZAP70*. A, Schematic ZAP70 with N-SH2 domain, C-SH2 domain and kinase domain. The position of exon 6 and M558 is shown in black. Arrows point c.703-1G>A and c.1674G>A variants. B, Sanger sequencing of the family. Wild type c.703-1 or c.1674 positions are highlighted in blue. Heterozygous c.703-1G>A or c.1674G>A variants were highlighted in red. C, Flow cytometric analysis of ZAP70 expression in T cells, $CD4^+$ T cells and $CD8^+$ T cells. Numbers in plots indicate the difference in mean fluorescence intensity.

Figure 4. Impaired functions of ZAP70 proteins in P116 cells transduced with ZAP70 mutants. A, Immunoblot analysis of P116 cells expressing $ZAP70^{WT}$, $ZAP70^{M558I}$ or $ZAP70^{\Delta exon\ 6}$ stimulated with CD3 cross-linking. B, Immunoblot analysis of whole-cell lysates and anti-CD3ζ chain immunoprecipitation.

Figure 5. Signal transduction through the TCR/CD3 complex in $CD4^+$ or $CD8^+$ T-cells. A, Calcium mobilization induced by CD3 cross-linking (left) and ionomycin (right) in $CD4^+$ T cells (gray, control; black, patient). B, Calcium mobilization in $CD8^+$ T cells. C, CFSE labeled proliferation induced by anti-CD3/CD28 (left) and PMA/ionomycin (right) in $CD4^+$ T cells. Numbers in plots indicate percent divided cells. D, CFSE labeled proliferation in $CD8^+$ T cells.

FIG 1.

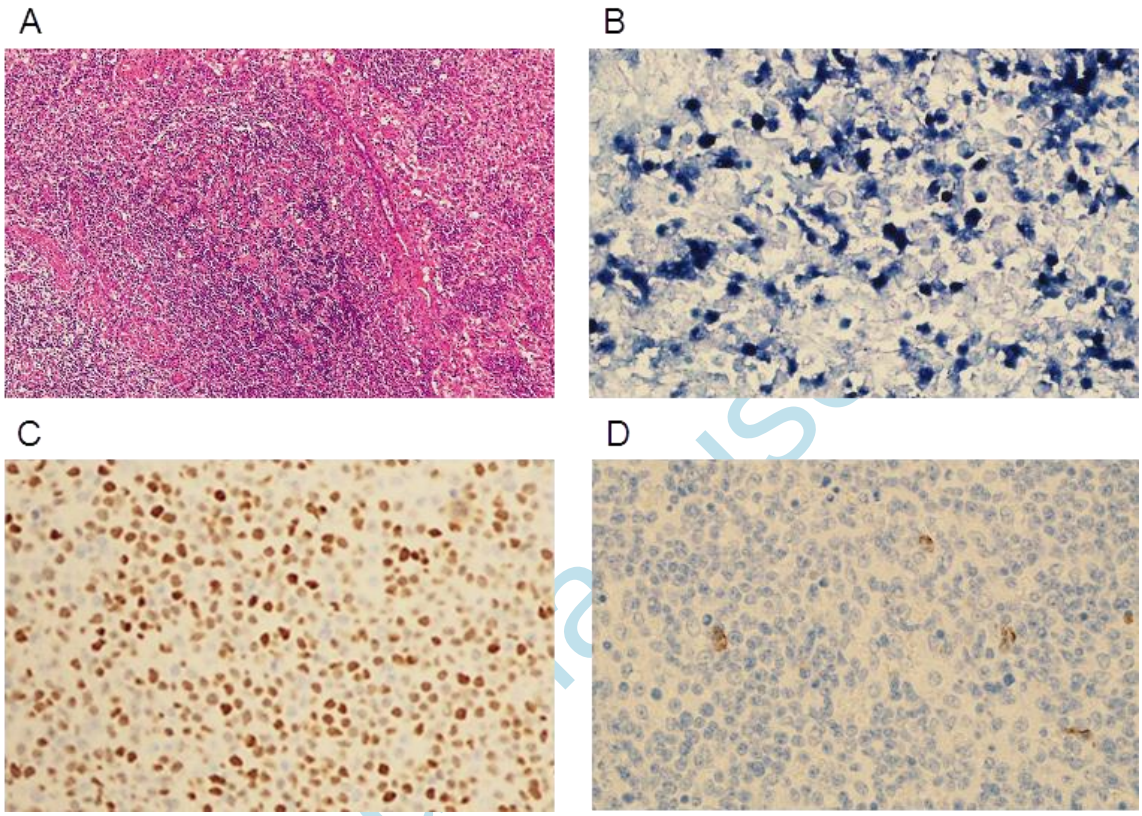

FIG 2.

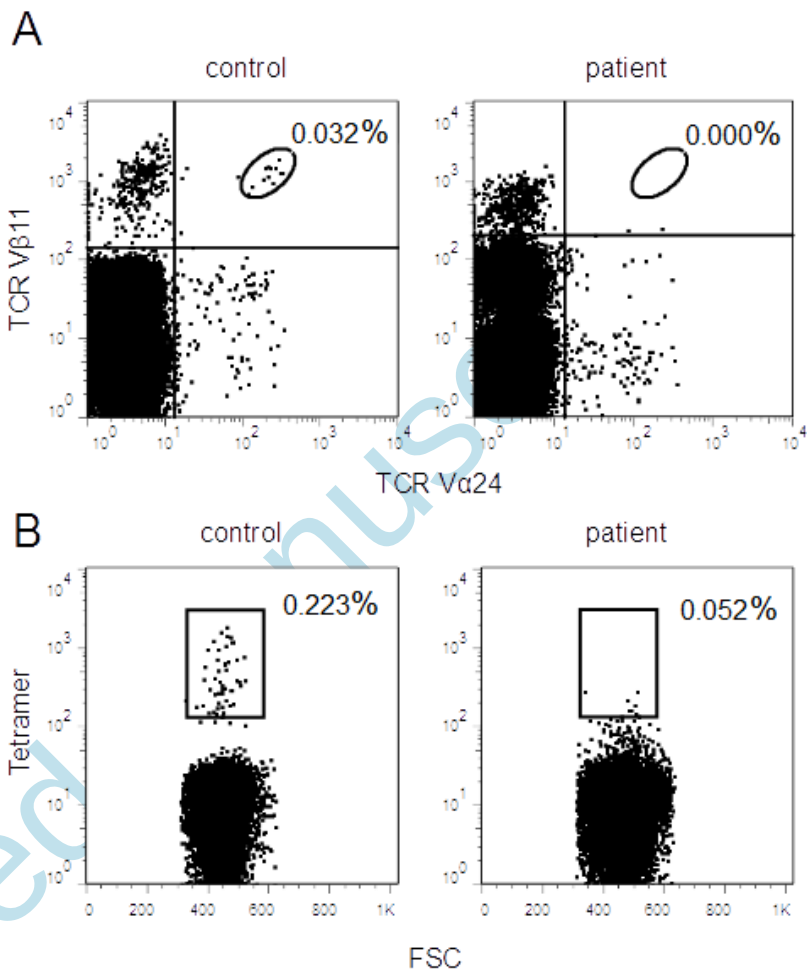

FIG 3.

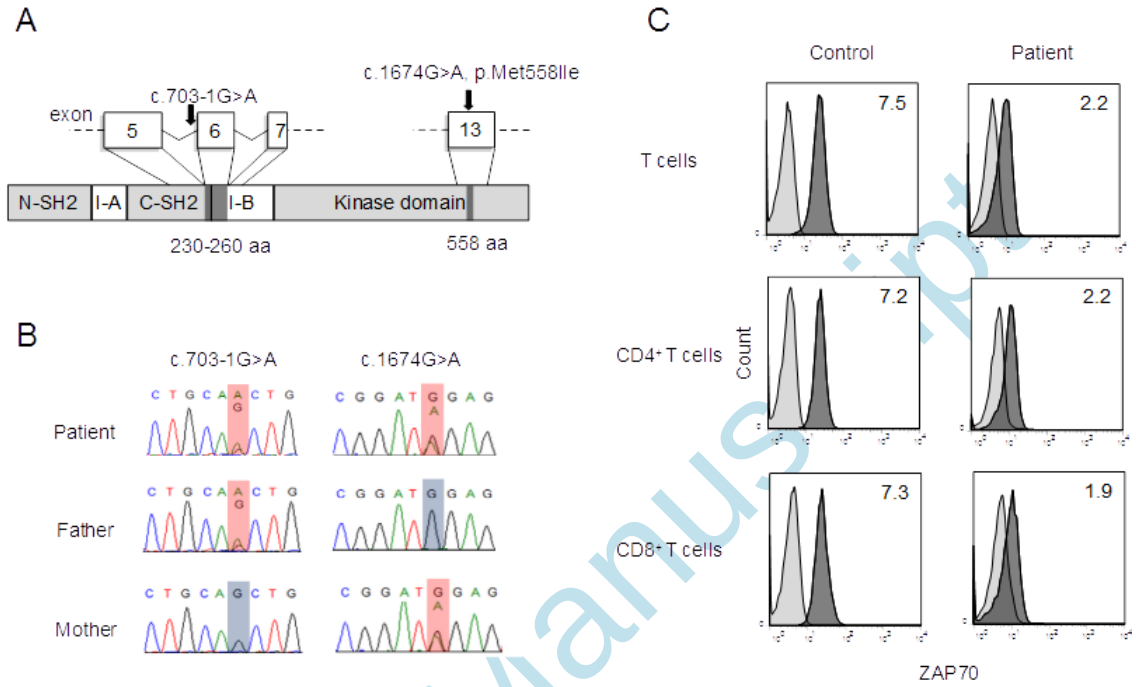

FIG 4.

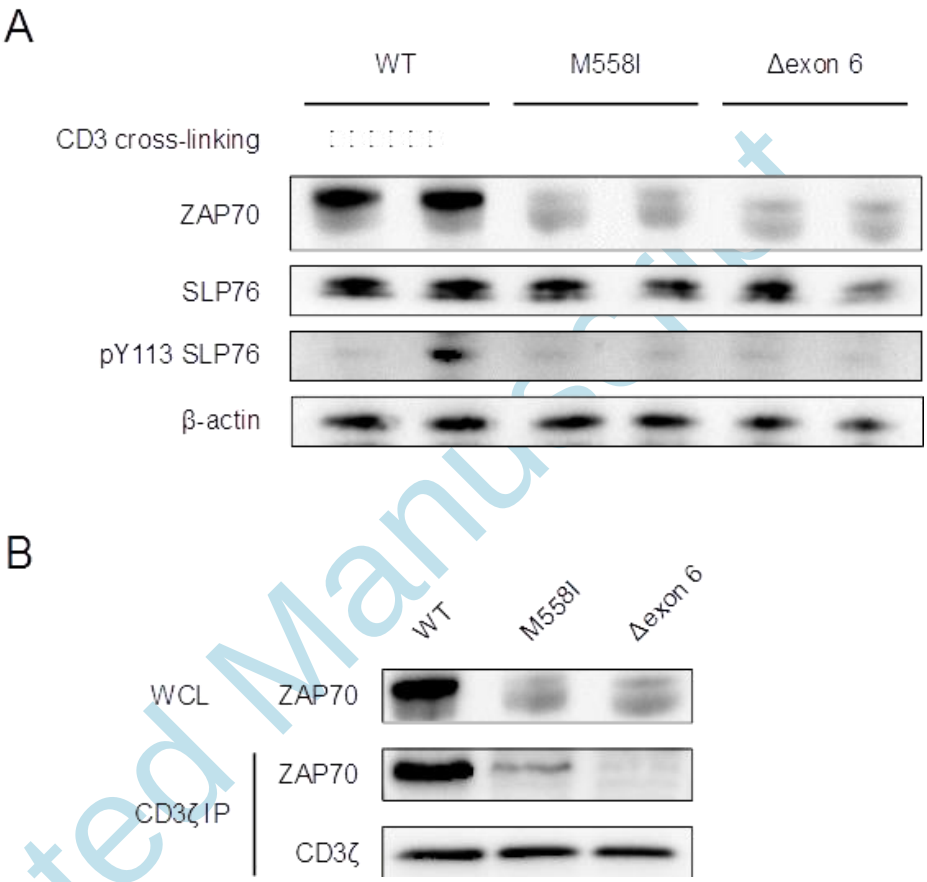

FIG 5.